

7U
S70/5i

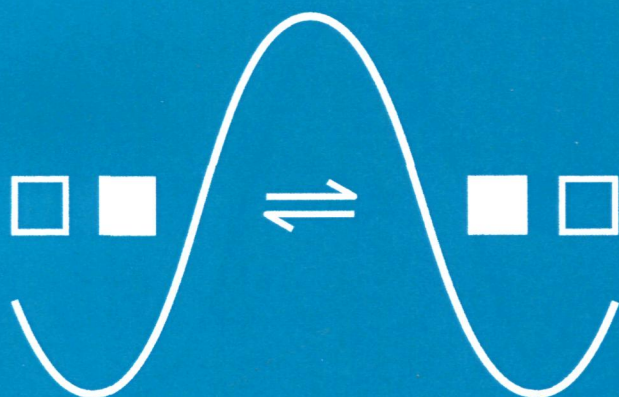
VOLUME 262, 1 September 2014

ISSN 0167-2738



SOLID STATE IONICS

DIFFUSION & REACTIONS



Proceedings of the 19th International Conference on
Solid State Ionics (SSI-19)

Guest Editors

M. Tatsumisago
M. Watanabe
K. Amezawa
Y. Iriyama
N. Kuwata
T. Omata
H. Matsumoto

Principal Editor

Joachim Maier, Stuttgart, Germany

Regional Editor Europe

John Kilner, London, UK

Regional Editor Asia

Koichi Eguchi, Kyoto, Japan
Hong Li, Beijing, China

Regional Editor USA

Arumugam Manthiram, Austin, TX, USA

Editors

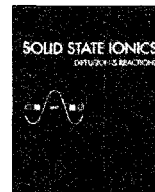
Klaus Funke, Münster, Germany
Truls Norby, Oslo, Norway
Josh Thomas, Uppsala, Sweden

Founding Editor

M. Stanley Whittingham, Binghamton, NY, USA

Editorial Assistant

Rotraut Merkle, Stuttgart, Germany



Contents

Special Issue

Proceedings of the 19th International Conference on Solid State Ionics (SSI-19)

Guest Editors: M. Tatsumisago, M. Watanabe, K. Amezawa, Y. Iriyama, N. Kuwata, T. Omata and H. Matsumoto

Editorial

The 19th International Conference on Solid State Ionics (SSI-19)

J. Mizusaki, S. Yamaguchi, K. Eguchi, T. Ishihara and M. Tatsumisago

1

Plenary

From Onsager to mixed ionic electronic conductors

T. Lee, H.-S. Kim and H.-I. Yoo

2

Battery: LIB

The effect of electrode thickness on electrochemical performance of LiMn_2O_4 cathode synthesized by modified sol-gel method

B. Hamankiewicz, M. Michalska, M. Krajewski, D. Ziolkowska, L. Lipinska, K. Korona, M. Kaminska and A. Czerwinski

9

Synthesis, crystal structure, and electrochemical properties of hollandite-type $\text{K}_x\text{Ti}_{1-y}\text{Mn}_y\text{O}_2$

N. Kijima, M. Sakao, Y. Tanuma, K. Kataoka, K. Igarashi and J. Akimoto

14

Negative electrode comprised of Fe_3O_4 nanoparticles and Cu nanowires for lithium ion batteries

F.-S. Ke, L. Jamison, L. Huang, B. Zhang, J.-T. Li, X.-D. Zhou and S.-G. Sun

18

Influence of pyrolysis atmosphere on the lithium storage properties of carbon-rich polymer derived SiOC ceramic anodes

V.S. Pradeep, M. Graczyk-Zajac, M. Wilamowska, R. Riedel and G.D. Soraru

22

Effect of carbon coating methods on structural characteristics and electrochemical properties of carbon-coated lithium iron phosphate

J.-K. Kim, D.-S. Kim, D.-H. Lim, A. Matic, G.S. Chauhan and J.-H. Ahn

25

The synthesis, characterization and electrochemical properties of $\text{V}_3\text{O}_7 \cdot \text{H}_2\text{O}/\text{CNT}$ Nanocomposite

Z. Li, H. Sun, J. Xu, Q. Zhu, W. Chen and G.S. Zakharova

30

Relaxation analysis of LiMnPO_4 -based olivine-type material

Y. Satou, S. Komine, S. Park and T. Yao

35

Effects of Li pre-doping on charge/discharge properties of Si thin flakes as a negative electrode for Li-ion batteries

T. Okubo, M. Saito, C. Yodoya, A. Kamei, M. Hirota, T. Takenaka, T. Okumura, A. Tasaka and M. Inaba

39

The effects of Al_2O_3 coating on the performance of layered $\text{Li}_{1.20}\text{Mn}_{0.55}\text{Ni}_{0.16}\text{Co}_{0.09}\text{O}_2$ materials for lithium-ion rechargeable battery

H. Kobayashi, T. Okumura, M. Shikano, K. Takada, Y. Arachi and H. Nitani

43

Experimental evaluation of LiFeTiO_4 as an electrode

S. Chakrabarti, A.K. Thakur and K. Biswas

49

Effect of microstructure on discharge properties of polycrystalline LiCoO_2

S. Yamakawa, H. Yamasaki, T. Koyama and R. Asahi

56

Synthesis and performance of apple-like tin oxide as anode for Li-ion batteries

P. Peng, Z. Wen, Y. Liu, Y. Lu, M. Wu, J. Jin, C. Liu and G. Ma

61

Evaluation of the effective reaction zone in a composite cathode for lithium ion batteries

T. Nakamura, T. Watanabe, K. Amezawa, H. Tanida, K. Ohara, Y. Uchimoto and Z. Ogumi

66

Numerical investigation of kinetic mechanism for runaway thermo-electrochemistry in lithium-ion cells

N. Tanaka and W.G. Bessler

70

Electronic structure of spinel-type $\text{LiNi}_{1/2}\text{Ge}_{3/2}\text{O}_4$ and $\text{LiNi}_{1/2}\text{Mn}_{3/2}\text{O}_4$ as positive electrodes for rechargeable Li-ion batteries studied by first-principles density functional theory

M. Nakayama, R. Jalel and T. Kasuga

74

| | |
|--|-----|
| Electrochemical characterization of poly(vinylidene fluoride-co-hexafluoro propylene) based electrospun gel polymer electrolytes incorporating room temperature ionic liquids as green electrolytes for lithium batteries P. Raghavan, X. Zhao, H. Choi, D.-H. Lim, J.-K. Kim, A. Matic, P. Jacobsson, C. Nah and J.-H. Ahn | 77 |
| Structure and electrochemical performance of the spinel-LiMn ₂ O ₄ synthesized by mechanical alloying T.Y.S.P. Putra, M. Yonemura, S. Torii, T. Ishigaki and T. Kamiyama | 83 |
| High-pressure synthesis of lithium-rich layered rock-salt Li ₂ (Mn _{3/8} Co _{1/4} Ni _{3/8})O _{3-x} for lithium battery cathodes Y. Matsuda, K. Suzuki, M. Hirayama and R. Kanno | 88 |
| Neutron diffraction studies on structural effect for Ni-doping in LiCo _{1-x} Ni _x O ₂ D.S. Adipranoto, T. Ishigaki, A. Hoshikawa, K. Iwase, M. Yonemura, K. Mori, T. Kamiyama, Y. Morii and M. Hayashi | 92 |
| Stability of C/Li ₂ MnSiO ₄ composite cathode material for Li-ion batteries towards LiPF ₆ based electrolyte M. Molenda, M. Świątosławski, A. Wach, D. Majda, P. Kuśtrowski and R. Dziembaj | 98 |
| Effects of V doping on the electrochemical performance of Li ₃ MnO ₄ for lithium ion batteries S. Xie, Z. Yu, H. Liu and S. Wu | 102 |
| Single-crystal growth, crystal structure analysis and physical properties of lithium overstoichiometric Li _{1+x} CoO ₂ K. Kataoka and J. Akimoto | 106 |
| Local structural change in Li ₂ FeSiO ₄ polyanion cathode material during initial cycling T. Mase, Y. Orikasa, T. Mori, K. Yamamoto, T. Ina, T. Minato, K. Nakanishi, T. Ohta, C. Tassel, Y. Kobayashi, H. Kageyama, H. Arai, Z. Ogumi and Y. Uchimoto | 110 |
| Structural changes and electrochemical properties of Li ₂ Cu _{1-x} M _x O ₂ for lithium secondary batteries E. Setiawati, M. Hayashi, M. Tsuda, K. Hayashi and R. Kobayashi | 115 |
| Low temperature molten salt synthesis of anatase TiO ₂ and its electrochemical properties M.V. Reddy, S. Adams, G.T.J. Liang, I.F. Mingze, H. Van Tu An and B.V.R. Chowdari | 120 |
| Structural and transport properties of Li _{1+x} V _{1-x} O ₂ anode materials for Li-ion batteries B. Gędziorowski, Ł. Kondracki, K. Świerczek and J. Molenda | 124 |
| Electrochemical properties of nano-sized binary metal oxides as anode electrode materials for lithium battery synthesized from layered double hydroxides Z. Quan, E. Ni, Y. Ogasawara and N. Sonoyama | 128 |
| Battery: Next generation | |
| Porous iron oxide coating on β'-alumina ceramics for Na-based batteries Y. Hu, Z. Wen and X. Wu | 133 |
| Application of graphite–solid electrolyte composite anode in all-solid-state lithium secondary battery with Li ₂ S positive electrode T. Takeuchi, H. Kageyama, K. Nakanishi, T. Ohta, A. Sakuda, T. Sakai, H. Kobayashi, H. Sakaebe, K. Tatsumi and Z. Ogumi | 138 |
| Composite positive electrode based on amorphous titanium polysulfide for application in all-solid-state lithium secondary batteries A. Sakuda, N. Taguchi, T. Takeuchi, H. Kobayashi, H. Sakaebe, K. Tatsumi and Z. Ogumi | 143 |
| Preparation of composite electrode with Li ₂ S–P ₂ S ₅ glasses as active materials for all-solid-state lithium secondary batteries T. Hakari, M. Nagao, A. Hayashi and M. Tatsumisago | 147 |
| Interface behavior between garnet-type lithium-ion-conducting solid electrolyte and lithium metal R. Sudo, Y. Nakata, K. Ishiguro, M. Matsui, A. Hirano, Y. Takeda, O. Yamamoto and N. Imanishi | 151 |
| Phase transformation of the garnet structured lithium ion conductor: Li ₇ La ₃ Zr ₂ O ₁₂ M. Matsui, K. Sakamoto, K. Takahashi, A. Hirano, Y. Takeda, O. Yamamoto and N. Imanishi | 155 |
| Aprotic Li–O ₂ cells: Gas diffusion layer (GDL) as catalyst free cathode and tetraglyme/LiClO ₄ as electrolyte J. Zeng, J.R. Nair, C. Francia, S. Bodoardo and N. Penazzi | 160 |
| Fabrication of thin-film lithium batteries with 5-V-class LiCoMnO ₄ cathodes N. Kuwata, S. Kudo, Y. Matsuda and J. Kawamura | 165 |
| Mesoporous carbon/sulfur composite with polyaniline coating for lithium sulfur batteries J. Jin, Z. Wen, G. Ma, Y. Lu and K. Rui | 170 |
| The enhanced performance of Li–S battery with P ₁₄ YRTFSI-modified electrolyte G. Ma, Z. Wen, J. Jin, M. Wu, G. Zhang, X. Wu and J. Zhang | 174 |
| Effects of intermediate layer on interfacial resistance for all-solid-state lithium batteries using lithium borohydride K. Takahashi, H. Maekawa and H. Takamura | 179 |
| High capacity all-solid-state Cu–Li ₂ S/Li ₆ PS ₅ Br/In batteries M. Chen, R.P. Rao and S. Adams | 183 |
| Preparation of hydroxide ion conductive KOH–ZrO ₂ electrolyte for all-solid state iron/air secondary battery A. Matsuda, H. Sakamoto, T. Kishimoto, K. Hayashi, T. Kugimiya and H. Muto | 188 |
| Microspherical Na ₂ Ti ₃ O ₇ prepared by spray-drying method as anode material for sodium-ion battery W. Zou, J. Li, Q. Deng, J. Xue, X. Dai, A. Zhou and J. Li | 192 |
| Free-standing Ni mesh with in-situ grown MnO ₂ nanoparticles as cathode for Li–air batteries Y. Yu, B. Zhang, Z.-L. Xu, Y.-B. He and J.-K. Kim | 197 |
| ⁷ Li NMR study of milling effects on instability of lithium-sites in lithium substituted silver niobate K. Nakamura, Y. Michihiro, C. Moriyoshi, Y. Kuroiwa and S. Wada | 202 |
| Sodium intercalation in Na _x CoO _{2-y} – Correlation between crystal structure, oxygen nonstoichiometry and electrochemical properties D. Baster, K. Dybko, M. Szot, K. Świerczek and J. Molenda | 206 |

| | |
|--|-----|
| Lithium conducting solid electrolyte $\text{Li}_{1+x}\text{Al}_x\text{Ge}_2-x(\text{PO}_4)_3$ membrane for aqueous lithium air battery D. Safanama, D. Damiano, R.P. Rao and S. Adams | 211 |
| Characterization of Prussian blue as positive electrode materials for sodium-ion batteries H. Minowa, Y. Yui, Y. Ono, M. Hayashi, K. Hayashi, R. Kobayashi and K. I. Takahashi | 216 |
| Capacitors | |
| Controllable synthesis of flowerlike $\alpha\text{-MnO}_2$ as electrode for pseudocapacitor application Rusi and S.R. Majid | 220 |
| RGO-wrapped MnO_2 composite electrode for supercapacitor application P.Y. Chan, Rusi and S.R. Majid | 226 |
| Evaluation of aluminium doped lanthanum ferrite based electrodes for supercapacitor design A. Rai, A.L. Sharma and A.K. Thakur | 230 |
| Synthesis and electrochemical properties of graphene/ V_2O_5 xerogels nanocomposites as supercapacitor electrodes J. Xu, H. Sun, Z. Li, S. Lu, X. Zhang, S. Jiang, Q. Zhu and G.S. Zakharova | 234 |
| Reactors | |
| Electrochemical oxygen separation using hydroxide ion conductive layered double hydroxides Y. Arishige, D. Kubo, K. Tadanaga, A. Hayashi and M. Tatsumisago | 238 |
| A numerical comparison of hydrogen absorption behaviors of uranium and zirconium cobalt-based metal hydride beds H. Yoo, W. Kim and H. Ju | 241 |
| Ceria-based substrates for CO_2 separation membranes S.G. Patrício, C.M.C. Soares, C.F.N. Santos, F.M.L. Figueiredo and F.M.B. Marques | 248 |
| Isothermal catalytic oxidation of diesel soot on Yttria-stabilized Zirconia E. Obeid, M.N. Tsampas, S. Jonet, A. Boréave, L. Burel, M.C. Steil, G. Blanchard, K. Pajot and P. Vernoux | 253 |
| Investigation of the Electrochemical Promotion of Catalysis origins on electrochemical catalysts with oxygen ion conductive supports: Isotopic labeling mechanistic studies M.N. Tsampas, F.M. Sapountzi, A. Boréave and P. Vernoux | 257 |
| The impact of sulfur contamination on the performance of $\text{La}_{0.6}\text{Sr}_{0.4}\text{Co}_{0.2}\text{Fe}_{0.8}\text{O}_{3-\delta}$ oxygen transport membranes Y. Alqaheem, A. Thursfield, G. Zhang and I.S. Metcalfe | 262 |
| Sensors | |
| Sensing performance of zirconia-based gas sensor using titania sensing-electrode added with palladium Y. Fujio, T. Sato and N. Miura | 266 |
| Influence of the V_2O_5 content of the catalyst layer of a non-Nernstian NH_3 sensor D. Schönauer-Kamin, M. Fleischer and R. Moos | 270 |
| CO_2 and SO_2 tolerant Fe-doped metal oxides for solid state gas sensors S. Mulmi, R. Kannan and V. Thangadurai | 274 |
| All-solid-state sensors used in drilling muds to prevent H_2S gas evolution on oil wells C. Bohnke, S. Lorant, V. Gunes, J.-Y. Botquelen and J. Breviere | 279 |
| NASICON-based acetone sensor using three-dimensional three-phase boundary and Cr-based spinel oxide sensing electrode H. Zhang, C. Yin, Y. Guan, X. Cheng, X. Liang and G. Lu | 283 |
| Detection of NO by pulsed polarization of Pt I YSZ S. Fischer, R. Pohle, E. Magori, M. Fleischer and R. Moos | 288 |
| High Performance Mixed-Potential Type NO_x Sensor Based On Stabilized Zirconia and Oxide Electrode G. Lu, Q. Diao, C. Yin, S. Yang, Y. Guan, X. Cheng and X. Liang | 292 |
| Electrolysis cells | |
| $\text{LaNb}_{0.84}\text{W}_{0.16}\text{O}_{4.08}$ as a novel electrolyte for high temperature fuel cell and solid oxide electrolysis applications M.A. Laguna-Bercero, R.D. Bayliss and S.J. Skinner | 298 |
| Stability of LSCF electrode with GDC interlayer in YSZ-based solid oxide electrolysis cell S.J. Kim and G.M. Choi | 303 |
| PEFC | |
| Functionalized mesoporous materials as new class high temperature proton exchange membranes for fuel cells S.P. Jiang | 307 |
| Design and investigation of dual-layer electrodes for proton exchange membrane fuel cells B. Zhao, L. Sun, R. Ran and Z. Shao | 313 |
| One-dimensional modeling and analysis for performance degradation of high temperature proton exchange membrane fuel cell using PA doped PBI membrane M. Kim, T. Kang, J. Kim and Y.-J. Sohn | 319 |
| Meso-structured organosilicas as fillers for Nafion® membranes N.C. Rosero-Navarro, E.M. Domingues, N. Sousa, P. Ferreira and F.M.L. Figueiredo | 324 |

| | |
|--|-----|
| Theoretical study on oxidation reaction mechanism on Au catalyst in direct alkaline fuel cell T. Ishimoto, H. Kazuno, T. Kishida and M. Koyama | 328 |
| Effects of type of graphite conductive filler on the performance of a composite bipolar plate for fuel cells K. Kang, S. Park and H. Ju | 332 |
| SOFC | |
| Anelastic properties of $\text{La}_{0.6}\text{Sr}_{0.4}\text{Co}_{1-y}\text{Fe}_y\text{O}_{3-6}$ at high temperatures Y. Kimura, J. Tolchard, M.-A. Einarsrud, T. Grande, K. Amezawa, M. Fukuhara, S.-i. Hashimoto and T. Kawada | 337 |
| Investigation on $\text{Pr}_{2-x}\text{Sr}_x\text{NiO}_{4+\delta}$ ($x = 0.3-1.0$) cathode materials for intermediate temperature solid oxide fuel cell S.S. Bhoga, A.P. Khandale and B.S. Pahune | 340 |
| Ex-solution of Ni nanoparticles in a $\text{La}_{0.2}\text{Sr}_{0.8}\text{Ti}_{1-x}\text{Ni}_x\text{O}_{3-\delta}$ alternative anode for solid oxide fuel cell B.H. Park and G.M. Choi | 345 |
| Oxygen exchange, thermochemical expansion and cathodic behavior of perovskite-like $\text{Sr}_{0.7}\text{Ce}_{0.3}\text{MnO}_{3-6}$ I. Kuritsyna, V. Sinityn, A. Melnikov, Yu. Fedotov, E. Tsipis, A. Viskup, S. Bredikhin and V. Kharton | 349 |
| Cation-ordered perovskite-type anode and cathode materials for solid oxide fuel cells K. Zheng, K. Świerczek, J. Bratek and A. Klimkiewicz | 354 |
| Electrochemical characterization of multi-element-doped ceria as potential anodes for SOFCs H.T. Handal and V. Thangadurai | 359 |
| The structural and electrical properties of $\text{Sr}_2\text{Ni}_{0.75}\text{Mg}_{0.25}\text{MoO}_6$ and its compatibility with solid state electrolytes E.A. Filonova, A.S. Dmitriev, P.S. Pikalov, D.A. Medvedev and E.Yu. Pikalova | 365 |
| A theoretical model for the electrical conductivity of core-shell nano-composite electrode of SOFC M. Chen, D. Liu and Z. Lin | 370 |
| Effects of transition metal addition on sintering and electrical conductivity of La-doped CeO_2 as buffer layer for doped LaGaO_3 electrolyte film J.-E. Hong, S. Ida and T. Ishihara | 374 |
| High surface reactivity of La/Sr-Co perovskite based cathode with cation nonstoichiometry A. Takeshita, S. Miyoshi, S. Yamaguchi, T. Kudo and Y. Sato | 378 |
| Cathode compatibility, operation, and stability of LaNbO_4 -based proton conducting fuel cells A. Magrasó, M.-L. Fontaine, R. Bredesen, R. Haugsrud and T. Norby | 382 |
| Preparation of nano-structured cathode for protonic ceramic fuel cell by bead-milling method H. Oda, T. Yoneda, T. Sakai, Y. Okuyama and H. Matsumoto | 388 |
| Oxygen isotope labeling method and oxygen reduction reaction mechanism of an SOFC cathode M. Nishi, H. Yokokawa, H. Kishimoto, K. Yamaji and T. Horita | 392 |
| Visualization of oxide ionic diffusion at SOFC cathode/electrolyte interfaces by isotope labeling techniques T. Horita, M. Nishi, T. Shimonosono, H. Kishimoto, K. Yamaji, M.E. Brito and H. Yokokawa | 398 |
| Effect of the oxide substrate on the nickel particle properties H. Kishimoto, A. Suzuki, T. Shimonosono, M. Nishi, K. Yamaji, M.E. Brito, H. Yokokawa, F. Munakata and T. Horita | 403 |
| Electrochemical analysis for anode-supported microtubular solid oxide fuel cells in partial reducing and oxidizing conditions H. Sumi, T. Yamaguchi, K. Hamamoto, T. Suzuki and Y. Fujishiro | 407 |
| Electrical conductivity of Gd-doped ceria film at low temperatures (300–500 °C) S.W. Kim, Y. Lee and G.M. Choi | 411 |
| Effect of Sr doping on structural, electrical and electrochemical properties of Nd_2CuO_4 for IT-SOFC application A.P. Khandale and S.S. Bhoga | 416 |
| Comparison of chromium poisoning among solid oxide fuel cell cathode materials E. Park, S. Taniguchi, T. Daio, J.-T. Chou and K. Sasaki | 421 |
| Electrical conductivity of barium substituted LSGM electrolyte materials for IT-SOFC Raghvendra, R.K. Singh and P. Singh | 428 |
| A quantitative analysis of influence of Ni particle size of SDC-supported anode on SOFC performance: Effect of particle size of SDC support K. Sugihara, M. Asamoto, Y. Itagaki, T. Takemasa, S. Yamaguchi, Y. Sadaoka and H. Yahiro | 433 |
| Delamination-resistant bi-layer electrolyte for anode-supported solid oxide fuel cells M.Y. Park, Y.-G. Jung and H.-T. Lim | 438 |
| Chemical reactivity between $\text{Ce}_{0.7}\text{RE}_{0.2}\text{Mo}_{0.1}\text{O}_2$ (RE = Y, Sm) and 8YSZ, and conductivity studies of their solid solutions K. Singh and V. Thangadurai | 444 |
| Oxidation properties of ferritic stainless steel in dual $\text{Ar-H}_2\text{-H}_2\text{O}$ /air atmosphere exposure with regard to SOFC interconnect application M. Stygar, T. Brylewski, A. Kruk and K. Przybylski | 449 |
| Effect of polarization on Sr and Zr diffusion behavior in LSCF/GDC/YSZ system F. Wang, M.E. Brito, K. Yamaji, D.-H. Cho, M. Nishi, H. Kishimoto, T. Horita and H. Yokokawa | 454 |
| Microstructure evolution of NiO-YSZ cermet during sintering S.-S. Liu, M. Koyama, S. Toh and S. Matsumura | 460 |
| Electrochemical performance and stability of electrolyte-supported solid oxide fuel cells based on Y-substituted SrTiO_3 ceramic anodes Q. Ma, B. Iwanschitz, E. Dashjav, A. Mai, F. Tietz and H.-P. Buchkremer | 465 |

Fundamentals

| | |
|--|-----|
| Structure of silver bromide doped chalcogenide glasses Y. Onodera, T. Usuki, T. Nasu and S. Kohara | 469 |
| First-principles analysis on proton diffusivity in La_3NbO_7 K. Kato, K. Toyoura, A. Nakamura and K. Matsunaga | 472 |
| Analysis of the ionic conductivity in lithium salt-containing ionic liquids based on the bond strength–coordination number fluctuation model M. Ikeda and M. Aniya | 476 |
| The study of the lithium ion motion in β -alumina single crystal by NMR spectroscopy M.T. Chowdhury, R. Takekawa, Y. Iwai, N. Kuwata and J. Kawamura | 482 |
| Modeling of electrical properties of grain boundaries in n-conducting barium titanate ceramics as a function of temperature and dc-bias W. Preis and W. Sitte | 486 |
| Phase changes in lithium amide–borohydride complexes under high pressure H. Yamawaki, H. Fujihisa, Y. Gotoh and S. Nakano | 490 |
| Frequency dependence of ionic conductivity in a two-dimensional system of Ag β -alumina O. Kamishima, Y. Iwai and J. Kawamura | 495 |
| Thermally stimulated depolarization current measurements in cubic and tetragonal yttria-stabilized zirconia N. Horiuchi, Y. Tsuchiya, K. Nozaki, M. Nakamura, A. Nagai and K. Yamashita | 500 |
| Molecular dynamics study on the nature of ferroelasticity and piezoconductivity of lanthanum cobaltite W. Araki, J. Malzbender and Y. Arai | 504 |
| Oxygen removal at grain boundaries in platinum films on YSZ G. Beck and C. Bachmann | 508 |
| Stable sites and diffusion pathways of interstitial oxide ions in lanthanum germanate K. Imaizumi, K. Toyoura, A. Nakamura and K. Matsunaga | 512 |

Anion conductors

| | |
|--|-----|
| Ionic and electronic conductivity of 3 mol% Fe_2O_3 -substituted cubic yttria-stabilized ZrO_2 (YSZ) and scandia-stabilized ZrO_2 (ScSZ) O. Bohnke, V. Gunes, K.V. Kravchyk, A.G. Belous, O.Z. Yanchevskii and O.I. V'Yunov | 517 |
| Zn as sintering aid for ceria-based electrolytes L.A. Villas-Boas, F.M.L. Figueiredo, D.P.F. de Souza and F.M.B. Marques | 522 |
| Oxygen relaxation and oxide ion conduction of $\text{Zr}_{0.8-x}\text{Ce}_x\text{Y}_{0.2}\text{O}_{1.9}$ ($x = 0, 0.3, 0.5$) M. Ozawa and K. Imura | 526 |
| Crystal structure and potential interstitial oxide ion conductivity of LnNbO_4 and $\text{LnNb}_{0.92}\text{W}_{0.08}\text{O}_{4.04}$ ($\text{Ln} = \text{La, Pr, Nd}$) C. Li, R.D. Bayliss and S.J. Skinner | 530 |
| Effect of fluorite phase on the electrical conductivity of $(\text{Sm}_{1-x}\text{Dy}_x)_2\text{Zr}_2\text{O}_7$ pyrochlore Y. Arachi and D. Nabeshima | 536 |
| Low-temperature phase transition phenomena for bismuth-substituted $\text{La}_2\text{Mo}_2\text{O}_9$ S. Takai, K. Chisaka, H. Kawaji, T. Yao and T. Esaka | 540 |
| Interstitial oxide ion conduction in $(\text{Sm}_{2-x}\text{Zr}_x)\text{Zr}_2\text{O}_7 + \delta$ A.V. Shlyakhtina, D.A. Belov, A.V. Knotko, I.V. Kolbanev, A.N. Streletskii and L.G. Shcherbakova | 543 |
| Oxygen tracer diffusion in single crystalline yttrium silicate C. Argirusis, G. Antonaropoulos, G. Sourkouni and F. Jomard | 548 |
| Relationship between crystal structure and oxide-ion conduction in $\text{Nd}_2\text{Zr}_2\text{O}_7$ and $\text{La}_2\text{Zr}_2\text{O}_7$ deduced by high-temperature neutron diffraction T. Hagiwara, K. Nomura and H. Yamamura | 551 |
| Oxide ion and electron transport properties in lanthanum silicate oxyapatite ceramics A. Mineshige, H. Mieda, M. Manabe, T. Funahashi, Y. Daiko, T. Yazawa, M. Nishi, K. Yamaji, T. Horita, K. Amezawa, K. Yashiro, T. Kawada and H. Yoshioka | 555 |

Cation conductors

| | |
|---|-----|
| Effects of Sn substitution on the properties of Li_4SiO_4 ceramic electrolyte S.B.R.S. Adnan and N.S. Mohamed | 559 |
| Fast H^+/Li^+ ion exchange in $\text{Li}_{0.30}\text{La}_{0.57}\text{TiO}_3$ nanopowder and films in water and in ambient air O. Bohnke, S. Lorant, M. Roffat and P. Berger | 563 |
| Synthesis and properties of Al-free $\text{Li}_{7-x}\text{La}_3\text{Zr}_2-x\text{Ta}_x\text{O}_{12}$ garnet related oxides R. Inada, K. Kusakabe, T. Tanaka, S. Kudo and Y. Sakurai | 568 |
| Improved lithium-ion transport in NASICON-type lithium titanium phosphate by calcium and iron doping G.F. Ortiz, M.C. López, P. Lavela, C. Vidal-Abarca and J.L. Tirado | 573 |
| Hetero-epitaxial growth of $\text{Li}_{0.17}\text{La}_{0.61}\text{TiO}_3$ solid electrolyte on LiMn_2O_4 electrode for all solid-state batteries S. Kim, M. Hirayama, K. Suzuki and R. Kanno | 578 |
| Electrical conductivity and dielectric permittivity of $\text{Cu}_6\text{AsS}_5\text{I}$ superionic crystals T. Šalkus, A. Kežionis, M. Ivanov, M.I. Kayla, M. Kranjčec, I.P. Studenyak and J. Banys | 582 |

| | |
|---|-----|
| Li diffusive behavior of garnet-type oxides studied by muon-spin relaxation and QENS H. Nozaki, M. Harada, S. Ohta, I. Watanabe, Y. Miyake, Y. Ikedo, N.H. Jalarvo, E. Mamontov and J. Sugiyama | 585 |
| Lithium ion conduction in tavorite-type LiMXO_4F (M-X: Al-P, Mg-S) candidate solid electrolyte materials R. Jalem, M. Nakayama and T. Kasuga | 589 |
| Charge carrier relaxation in solid V_2O_5 conductors S. Kazlauskas, A. Kežionis, T. Šalkus and A.F. Orliukas | 593 |
| Influence of grain size effect on electrical properties of $\text{Cu}_6\text{PS}_5\text{I}$ superionic ceramics T. Šalkus, E. Kazakevičius, J. Banys, M. Kranjčec, A.A. Chomolyak, Yu.Yu. Neimet and I.P. Studenyak | 597 |
| Preparation of magnesium ion conducting $\text{MgS-P}_2\text{S}_5\text{-MgI}_2$ glasses by a mechanochemical technique T. Yamanaka, A. Hayashi, A. Yamauchi and M. Tatsumisago | 601 |
| Synthesis and Na^+ conduction properties of Nasicon-type glass-ceramics in the system $\text{Na}_2\text{O-Y}_2\text{O}_3\text{-R}_2\text{O}_3\text{-P}_2\text{O}_5\text{-SiO}_2$ (R = rare earth) and effect of Y substitution T. Okura, K. Kawada, N. Yoshida, H. Monma and K. Yamashita | 604 |
| Garnet-type $\text{Li}_{6.75}\text{La}_3\text{Zr}_{1.75}\text{Nb}_{0.25}\text{O}_{12}$ synthesized by coprecipitation method and its lithium ion conductivity H. Imagawa, S. Ohta, Y. Kihira and T. Asaoka | 609 |
| Improvement of electrochemical properties of LiFePO_4 fine particles synthesized in ethylene glycol solution resulting from heat treatment S. Fujieda, K. Shinoda and S. Suzuki | 613 |
| Synthesis procedure and effect of Nd, Ca and Nb doping on structure and electrical conductivity of $\text{Li}_7\text{La}_3\text{Zr}_2\text{O}_{12}$ garnets E. Hanc, W. Zajac and J. Molenda | 617 |
| Pressure dependence of crystal structure of Cu_2O by TOF powder neutron diffraction Y. Ishikawa, T. Sakuma, H. Takahashi and S.A. Danilkin | 622 |
| Mixed conductors | |
| Oxygen vacancy redistribution in $\text{PbZr}_x\text{Ti}_{1-x}\text{O}_3$ (PZT) under the influence of an electric field G. Holzlechner, D. Kastner, C. Slouka, H. Hutter and J. Fleig | 625 |
| Chemistry, structure and properties of bismuth copper titanate pyrochlores I.V. Piir, M.S. Koroleva, Yu.I. Ryabkov, E.Yu. Pikalova, S.V. Nekipelov, V.N. Sivkov and D.V. Vyalikh | 630 |
| <i>In situ</i> Hall effect and conductivity measurements of ITO thin films M.V. Hohmann, A. Wachau and A. Klein | 636 |
| Microstructure and electrical properties of the composites based on $\text{SrTi}_{0.5}\text{Fe}_{0.5}\text{O}_{3-\delta}$ and $\text{Ce}_{0.8}(\text{Sm}_{0.8}\text{Sr}_{0.2})_{0.2}\text{O}_{2-\delta}$ E.Yu. Pikalova, A.A. Murashkina, D.A. Medvedev, P.S. Pikalov and S.V. Plaksin | 640 |
| Correlation between crystal and transport properties in $\text{LnBa}_{0.5}\text{Sr}_{0.5}\text{Co}_{1.5}\text{Fe}_{0.5}\text{O}_{5+\delta}$ (Ln - selected lanthanides, Y) K. Świerczek, N. Yoshikura, K. Zheng and A. Klimkowicz | 645 |
| Stabilization of cubic perovskite structure upon trivalent cation substitution in Co-based mixed conductors $(\text{Ba}_x\text{Sr}_{1-x})(\text{Co}_{0.9}\text{Y}_{0.1})\text{O}_{3-\delta}$ T. Nagai and W. Ito | 650 |
| Directional solidification of $\text{ZrO}_2\text{-BaZrO}_3$ composites with mixed protonic-oxide ionic conductivity R.G. Carvalho, A.J.S. Fernandes, R.F. Silva, F.M. Costa and F.M. Figueiredo | 654 |
| Evaluation of $\text{BaY}_{1-x}\text{Pr}_x\text{Mn}_2\text{O}_{5+\delta}$ oxides for oxygen storage technology A. Klimkowicz, K. Świerczek, K. Zheng, M. Baranowska, A. Takasaki and B. Dabrowski | 659 |
| Oxygen permeation and oxide ion conductivity of Ta-substituted (La, Sr) $\text{CoO}_{3-\delta}$ I. Kagomiya, Y. Shimono and K.-i. Kakimoto | 664 |
| Oxygen surface exchange kinetics on $\text{PrBaCo}_2\text{O}_{5+\delta}$ C.-Y. Yoo, B.A. Boukamp and H.J.M. Bouwmeester | 668 |
| Structure and transport properties of $\text{La}_{0.5}\text{Sr}_{0.5-x}\text{Ca}_x\text{FeO}_{3-\delta}$ K.Yu. Chesnokov, A.A. Markov, M.V. Patrakeev, I.A. Leonidov, A.M. Murzakaev, O.N. Leonidova, E.V. Shalaeva, V.V. Kharton and V.L. Kozhevnikov | 672 |
| Temperature activated electron transport in CaMnO_3 E.I. Goldyreva, I.A. Leonidov, M.V. Patrakeev and V.L. Kozhevnikov | 678 |
| Crystal structure of $\text{Nd}_2\text{NiO}_{4.08}$ K. Ishikawa | 682 |
| Dependence of lattice constant of Ba, Co-contained perovskite oxides on atmosphere, and measurements of water content D. Hashimoto, D. Han and T. Uda | 687 |
| Preparation and electrode properties of composite cathodes based on $\text{Bi}_{1-x}\text{Sr}_x\text{FeO}_{3-\delta}$ with Perovskite-type structure D. Baek, A. Kamegawa and H. Takamura | 691 |
| Simulation of oxygen diffusion process on electrical conductivity relaxation H. Kudo, K. Yashiro, S.-i. Hashimoto, K. Amezawa and T. Kawada | 696 |
| Influence of synthesis route on electrical and electrochemical properties of $\text{Nd}_{1.8}\text{Sr}_{0.2}\text{NiO}_{4+\delta}$ J.D. Punde, A.P. Khandale and S.S. Bhoga | 701 |
| Oxygen mobility and surface reactivity of $\text{PrNi}_{1-x}\text{Co}_x\text{O}_{3+\delta}\text{-Ce}_{0.9}\text{Y}_{0.1}\text{O}_{2-\delta}$ cathode nanocomposites V. Sadykov, N. Eremeev, G. Alikina, E. Sadovskaya, V. Muzykantov, V. Pelipenko, A. Bobin, T. Krieger, V. Belyaev, V. Ivanov, A. Ishchenko, V. Rogov, A. Ulihin, N. Uvarov, Yu. Okhlupin, J. Mertens and I. Vinke | 707 |
| Zr-doped samarium molybdates – potential mixed electron-proton conductors S.N. Savvin, A.V. Shlyakhtina, I.V. Kolbanev, A.V. Knotko, D.A. Belov, L.G. Shcherbakova and P. Nuñez | 713 |

| | |
|---|-----|
| Effect of Nb doping on the chemical stability of BSCF-based solid solutions F. Wang, T. Nakamura, K. Yashiro, J. Mizusaki and K. Amezawa | 719 |
| Analysis of structural phase transition behavior of $\text{Ln}_2\text{NiO}_{4+\delta}$ (Ln: Nd, Pr) with variation of oxygen content E. Niwa, K. Wakai, T. Hori, T. Nakamura, K. Yashiro, J. Mizusaki and T. Hashimoto | 724 |
| Polymers, ionic liquids, and glasses | |
| Nanocrystallite effects on ion transport in molybdophosphate glasses B. Deb and A. Ghosh | 728 |
| A new lithium-ion conducting glass ceramic in the composition of $75\text{Li}_2\text{S} \cdot 5\text{P}_2\text{S}_3 \cdot 20\text{P}_2\text{S}_5$ (mol%) Y. Ooura, N. Machida, T. Uehara, S. Kinoshita, M. Naito, T. Shigematsu and S. Kondo | 733 |
| Polycarbonate-based solid polymer electrolytes for Li-ion batteries B. Sun, J. Mindemark, K. Edström and D. Brandell | 738 |
| Electronic structure of silver halide doped glasses T. Awano | 743 |
| A single-ion gel polymer electrolyte based on polymeric lithium tartaric acid borate and its superior battery performance X. Wang, Z. Liu, Q. Kong, W. Jiang, J. Yao, C. Zhang and G. Cui | 747 |
| Anion conductive aromatic membrane of poly(tetra phenyl ether sulfone) containing hexa-imidazolium hydroxides for alkaline fuel cell application M.A. Hossain, Y. Lim, S. Lee, H. Jang, S. Choi, Y. Jeon, S. Lee, H. Ju and W.G. Kim | 754 |
| Cross-linked poly(oxetane) matrix for polymer electrolyte containing lithium ions H. Tsutsumi and A. Suzuki | 761 |
| Development of high capacity all-solid-state lithium battery using quasi-solid-state electrolyte containing tetraglyme–Li-TFSA equimolar complexes A. Unemoto, Y. Gambe, D. Komatsu and I. Honma | 765 |
| Molecular dynamics modeling the Li-PolystyreneTFSI/PEO blend D. Brandell, H. Kasemägi, T. Tamm and A. Aabloo | 769 |
| Ionic conductive properties of solid polymer electrolyte based on poly(oxetane) with branched side chains of terminal nitrile groups Y. Nakano and H. Tsutsumi | 774 |
| Mixed glass former effect in AgI doped silver borophosphate glasses S. Kabi and A. Ghosh | 778 |
| Design of superionic polymers—New insights from Walden plot analysis Y. Wang, F. Fan, A.L. Agapov, X. Yu, K. Hong, J. Mays and A.P. Sokolov | 782 |
| Relation between structural and conductivity relaxation in PEO and PEO based electrolytes B. K. Money, K. Hariharan and J. Swenson | 785 |
| Ionic liquid assisted modification in ionic conductivity, phase transition temperature and crystallization kinetics behaviour of polymer poly(ethylene oxide) S.K. Chaurasia, R.K. Singh and S. Chandra | 790 |
| π -Conjugated polycarbazole–boron complex as a colorimetric fluoride ion sensor R. Vedarajan, Y. Hosono and N. Matsumi | 795 |
| Electronic conductivity in the SiO_2 – PbO – Fe_2O_3 glass containing magnetic nanostructures R.J. Barczyński, N.A. Szreder, J. Karczewski and M. Gazda | 801 |
| Ion dynamics behavior in solid polymer electrolyte N. Srivastava and M. Kumar | 806 |
| PVDF supported silica immobilized phosphotungstic acid membrane for DMFC application J. Pandey and A. Shukla | 811 |
| Evidence of low temperature relaxation and hopping in ion conducting polymer blend A. Das, A.K. Thakur and K. Kumar | 815 |
| ^{108}mAg tracer diffusion in HgI_2 – Ag_2S – As_2S_3 glass system R. Boidin, I. Alekseev, K. Michel, D. Le Coq and E. Bychkov | 821 |
| Mixed alkali effect on crystallization kinetics of $x\text{Na}_2\text{O}:(50-x)\text{Li}_2\text{O}:50\text{P}_2\text{O}_5$ B. K. Money and K. Hariharan | 824 |
| Li-ion conductive phosphosilicate glass ceramics synthesized by ion exchange T. Tsujimura | 829 |
| Structure and dynamics of solid electrolyte $(\text{LiI})_{0.3}(\text{LiPO}_3)_{0.7}$ E. Kartini, M. Nakamura, M. Arai, Y. Inamura, K. Nakajima, T. Maksun, W. Honggowiranto and T.Y.S.P. Putra | 833 |
| Electrical properties and structure of lead-borate glass containing iron ions N.A. Szreder, R.J. Barczyński, J. Karczewski and M. Gazda | 837 |
| Proton conductors | |
| Neutron diffraction study of LaScO_3 -based proton conductor K. Nomura and H. Kageyama | 841 |
| Synthesis and characterization of sulfonated cardo based poly(arylene ether sulfone) multiblock copolymers for proton exchange membrane H. Jang, M.M. Islam, Y. Lim, S. Lee, M.A. Hossain, T. Hong, S. Lee, Y. Hong and W.-G. Kim | 845 |

| | |
|---|-----|
| Chemical solution deposition of thin films for protonic ceramic fuel cells P.M. Rørvik, C. Haavik, D. Griesche, T. Schneller, F. Lenrick and L.R. Wallenberg | 852 |
| Proton conducting tungsten phosphate glass and its application in intermediate temperature fuel cells T. Ishiyama, S. Suzuki, J. Nishii, T. Yamashita, H. Kawazoe and T. Omata | 856 |
| High spatially resolved cation concentration profile at the grain boundaries of Sc-doped BaZrO ₃ M. Shirpour, G. Gregori, L. Houben, R. Merkle and J. Maier | 860 |
| Incorporation of a proton into La _{0.9} Sr _{0.1} (Yb _{1-x} M _x)O _{3-δ} (M = Y, In) Y. Okuyama, S. Ikeda, T. Sakai and H. Matsumoto | 865 |
| Combined bulk and surface analysis of the BaCe _{0.5} Zr _{0.3} Y _{0.16} Zn _{0.04} O _{3-δ} (BCZYZ) ceramic proton-conducting electrolyte A. Ślodyczyk, M.D. Sharp, S. Upasen, P. Colomban and J.A. Kilner | 870 |
| Percolation conductivity in BaZrO ₃ -BaFeO ₃ solid solutions D. Kim, S. Miyoshi, T. Tsuchiya and S. Yamaguchi | 875 |
| Nanoscale ionic phenomena & manipulation | |
| Interfacial phenomena between lithium ion conductors and cathodes H. Yamada, K. Suzuki, K. Nishio, K. Takemoto, G. Isomichi and I. Moriguchi | 879 |
| Examining the crossing of I-V curves in devices based on mixed-ionic-electronic-conductors D. Kalaev and I. Riess | 883 |
| Oxide ionic conductivity in Pr ₂ (Ni, Cu, Ga)O _{4+δ} -(Ce, Sm)O _{2-δ} laminated film estimated with the Hebb-Wagner method J. Hyodo, S. Ida and T. Ishihara | 889 |
| New tools for SSI | |
| Surface composition of perovskite-type materials studied by Low Energy Ion Scattering (LEIS) J. Druce, T. Ishihara and J. Kilner | 893 |
| Assessing the identifiability in isotope exchange depth profiling measurements F. Ciucci, G. Panagakos, C. Chen and D. Chen | 897 |
| Lithium diffusive behavior in Li ₂ MnO ₃ detected by muon-spin relaxation J. Sugiyama, H. Nozaki, K. Mukai, M. Harada, M. Månsson and A. Hillier | 901 |
| Optical absorption of electronic defects and chemical diffusion in vapor transport equilibrated lithium niobate at high temperatures J. Shi, H. Fritze, A. Weidenfelder, C. Swanson, P. Fielitz, G. Borchardt and K.-D. Becker | 904 |
| Rapid hydrogen production from water using aluminum nanoclusters: A quantum molecular dynamics simulation study P. Vashishta, F. Shimojo, S. Ohmura, K. Shimamura, W. Mou, R.K. Kalia and A. Nakano | 908 |
| Development of in situ soft X-ray absorption spectroscopic technique under high temperature and controlled atmosphere R. Oike, K. Amezawa, T. Nakamura, Y. Tamenori, K. Yashiro and T. Kawada | 911 |
| Electrical conductivity relaxation measurements: Application of low thermal mass heater stick D. Chen, A. Groß, D.C. Bono, J. Kita, R. Moos and H.L. Tuller | 914 |
| In situ X-ray diffraction studies of Pr _{2-x} NiO _{4+δ} crystal structure relaxation caused by oxygen loss V. Sadykov, Yu. Okhlupin, N. Yermeev, Z. Vinokurov, A. Shmakov, V. Belyaev, N. Uvarov and J. Mertens | 918 |